Smart Structures and Systems, Vol. 9, No. 2 (2012) 189-206
DOI: http://dx.doi.org/10.12989/sss.2012.9.2.189

Electrically-induced actuation for open-loop control to cancel self-excitation vibration

Kanjuro Makihara*[1] and Horst Ecker[2]

[1]*Department of Aerospace Engineering, Tohoku University, 6-6-01 Aoba Aramaki Aoba-ku, Sendai 980-8579, Japan*
[2]*Institute of Mechanics and Mechatronics, Vienna University of Technology, Wiedner Hauptstrasse 8, Vienna A-1040, Austria*

(Received January 24, 2011, Revised February 1, 2012, Accepted February 2, 2012)

Abstract. This paper focuses on the actuation system combined with a piezoelectric transducer and an electric circuit, which leads to a new insight; the electric actuation system is equivalent to mechanical variable-stiffness actuation systems. By controlling the switch in the circuit, the electric status of the piezoelectric transducer is changed, and consequently a variable-stiffness mechanism is achieved on the electric actuator. This proposed actuator features a shift in the equilibrium point of force, while conventional electrically-induced variable-stiffness actuators feature the variation of the stiffness value. We intensively focus on the equilibrium shift in the actuation system, which has been neglected. The stiffness of the variable-stiffness actuator is periodically modulated by controlling the switch, to suppress the vibration of the system in an open-loop way. It is proved that this electric actuator is equivalent to its mechanical counterpart, and that the electrical version has some practical advantages over the mechanical one. Furthermore, another kind of electrically-induced variable-stiffness actuator, using an energy-recycling mechanism is also discussed from the viewpoint of open-loop vibration control. Extensive numerical simulations provide comprehensive assessment on both electrically-induced variable-stiffness actuators employed for open-loop vibration control.

Keywords: stiffness-variable actuator; piezoelectric; open-loop control; switching control; semi-active.

1. Introduction

Any structure is vulnerable to extensive vibrations that can cause its failure and reduce its life. There is currently a large effort underway to attenuate the vibration of structures. In general, vibration control methods can be categorized as closed-loop methods or as open-loop methods. Unlike closed-loop methods, open-loop methods do not need to have sensors, filters or processors, which reduces the practical cost and makes the system more feasible and reliable. As for an open-loop vibration control, an innovative method using parametric excitations was proposed (Tondl 1998). Within a certain control frequency interval, parametric excitation induces a parametric anti-resonance, and the anti-resonance mechanism cancels self-excited vibrations. This method was applied to systems subject to flow-induced self-excitation and to friction-induced self-excitation (Tondl and Ecker 2003, Ecker and Pumhossel 2009). In these studies, the parametric excitation was realized by periodically changing the stiffness coefficient of a linear spring. In particular, vibration canceling of a vibrating

*Corresponding author, Associate Professor, E-mail: makihara@ssl.mech.tohoku.ac.jp

structure was achieved by employing four types of mechanical variable-stiffness actuators, and their vibration canceling mechanisms was clarified (Makihara *et al.* 2005).

There have been many studies on the synthesis of piezoelectric materials and electric devices to suppress structural vibrations. Piezoelectric materials attached to or embedded in structures can convert mechanical energy into electrical energy, or *vice versa.* They have been extensively utilized as actuators, sensors, and transducers for various purposes. The proposed actuation method uses a combination of a piezoelectric transducer and a passive electric circuit having a switch. Therefore, a short introduction to recent works on vibration controls using this combination is made here. In their studies, the circuit switch is closed or opened to suppress vibrations. Clark (2000) has proposed a state-switching method implemented with a switchable stiffness element. When a mass is moving towards an equilibrium point, a piezoelectric transducer is short-circuited, while when the mass is moving away from the equilibrium point, the transducer is open-circuited. A theoretical analysis of the suppression performance capacity of the state-switching method was provided (Kurdila *et al*. 2006). A "switched stiffness" vibration control was proposed with an output feedback variable structure observer, so that the suppression performance would not degraded by the intervention of noise and the resulting signal phase-lag due to filters (Ramaratnam *et al.* 2006). In effect, the electrical state of the piezoelectric transducer is changed every quarter cycle. This quarter-cycle switching leads to the generation of potentially undesirable mechanical transients (Cunefare *et al*. 2000). To avoid the undesirable phenomenon, a state-switched vibration absorber (SSA) was proposed (Larson and Cunefare 2004). The SSA is switched at conditions of zero strain across the switchable element.

As will be discussed later, these preceding studies focused only on the variation of the stiffness value, not on the shift in the equilibrium point of force. This paper intends to point out that the piezoelectric actuator has a crucial mechanism of the equilibrium point's shift, which has been neglected so far.

2. Mechanical energy-dissipation (MED) actuator

The work in this paper is based on our previous research (Makihara *et al*. 2005) on a mechanical variable-stiffness actuator that has an energy-dissipation mechanism. A brief introduction to the

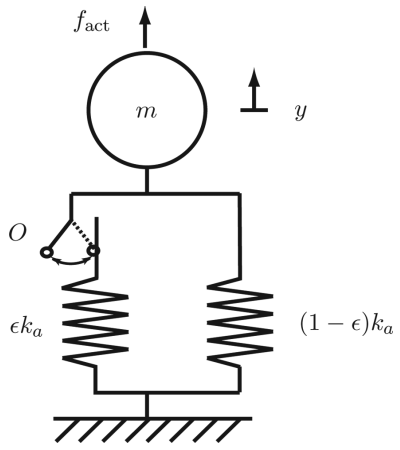

Fig. 1 Mechanical variable-stiffness actuator modeled with primary spring (1-ε)k_a and secondary spring εk_a

mechanical variable-stiffness actuator is given by using a simple model of a mass m shown in Fig. 1. The mechanical variable-stiffness actuator can be built from two springs and an attaching device. The primary spring (spring constant: $(1-\varepsilon)k_a$) is always connected to the mass at one end. The secondary spring (spring constant: εk_a) is attached to or detached from the mass by the attaching device (O). Depending on the status of the attaching device, the actuator takes on one of the two stiffness values k_a or $(1-\varepsilon)k_a$ [variable-stiffness feature 1]. Since the attaching device can be reconnected to the the secondary spring in the neutral-length state where the secondary spring does not stretch or shrink, the reconnection does not require external energy. This leads to the fact that any action of the attaching device does not increase the energy of the system. When the attaching device detaches the secondary spring from the mass, the vibration energy of the system will be converted in the secondary spring, and in consequence, will be dissipated in the local free vibration of the secondary spring due to its damping property.

Fig. 2 schematically shows force on the variable-stiffness actuator f_{act} against displacement y. At $y=y_0$, force jumps from point A to point B, as stiffness suddenly decreases, but remains at point B even when stiffness suddenly increases. This time, when stiffness increases again, the state moves along line BC. This mechanical variable-stiffness actuator can shift its equilibrium point of force from $y_{ep} = 0$ to $y_{ep} = \varepsilon y_0$. When the secondary spring is detached from the mass,

$$f_{act} = (1 - \varepsilon)k_a y \tag{1}$$

When the secondary spring is attached to the mass

$$f_{act} = k_a y - \varepsilon k_a y_0 \tag{2}$$

where y_0 is the displacement of the mass just when the secondary spring is reconnected. When the attaching point changes from attaching state to detaching state (point A to B in 2 Fig. 2), an energy of $\varepsilon k_a y_0^2/2$ will be converted in the secondary spring and will be dissipated eventually. Here, the detail explanation of the energy dissipation is presented. The secondary spring (εk_a) inherently has both the mass and the dash-pot element that can dissipate energy. The mass and dash-pot of the secondary spring is not depicted explicitly in the Fig. 1, to avoid unnecessary confusion. After the secondary spring is

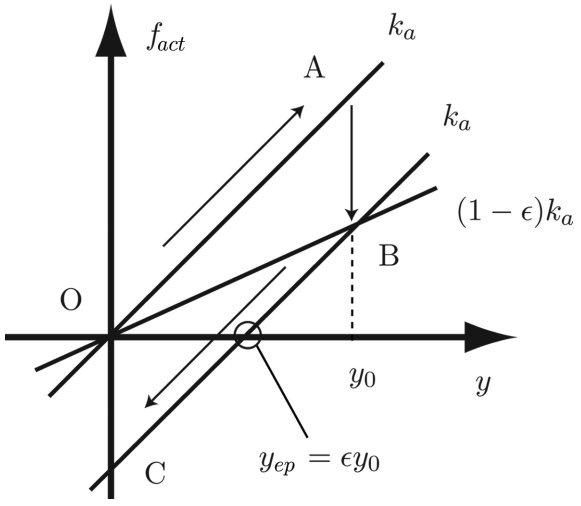

Fig. 2 Force-displacement chart for mechanical variable-stiffness actuator

detached from the mass, it starts to vibrate freely, because it has elastic energy. During the process with the dash-pot element, the vibration energy of secondary spring dissipated. Finally, the secondary spring turns back to its neutral position with its neutral length.

In contrast, when the attaching device changes from detaching state to attaching state (remaining point B), the vibration energy of the system will be unchanged. In summary, the variable-stiffness actuator's equilibrium point of force can shift when the secondary spring is detached from the mass and is again reattached to the mass [variable-stiffness feature 2].

In this research, an open-loop variable-stiffness control (Makihara *et al.* 2005) is adopted. The control logic based on the following rules is introduced: the duration when the mechanical energy is stored into the secondary spring should be as long as possible, and the releasing time should be made as short as possible. This control scheme was referred to as Logic 2B in our previous study (Makihara *et al*. 2005). This control logic tries to minimize the idle duration while the secondary spring dissipates its transferred energy. The secondary spring is detached from the structure for a very short period Δt_m at the time $t = 2n\pi/\omega$ ($n \in \mathbf{Z}$). ω is the open-loop control frequency that is determined in advance. This open-loop control is based on the actuator's force in Fig. 2 as

$$f_{act} = k_a(1-\varepsilon)y \qquad \text{during } \Delta t_m \text{ just after } t = 2n\pi/\omega \tag{3}$$

$$f_{act} = k_a\, y - \varepsilon k_a y_0 \qquad \text{otherwise} \tag{4}$$

The mechanical variable-stiffness actuator whose stiffness is modulated according to the control logic given by Eqs. (3) and (4) possesses a mechanical energy-dissipation mechanism. Therefore, in this paper, it is referred to as MED (mechanical energy-dissipation) actuator. Δt_m should be large enough for the vibration decay of local free vibrations of the secondary spring.

Since this MED actuator has a stiffness value of k_a most of the control time, the variable stiffness feature 1 has little influence on the performance of open-loop vibration control. On the other hand, the variable-stiffness feature 2 leads to the hysteresis in displacement-force chart, which results in an energy-dissipation mechanism. The feature 2 of the MED actuator has great effect on the performance of open-loop vibration control.

3. Problem statement and research objective

The MED actuator as shown in Fig. 1 was built for experiments of closed-loop vibration control (Onoda *et al.* 1991). In the experiments, the secondary spring has an attaching device that can extrude in the direction perpendicular to the vibrating direction, in order to attach the second spring to the structure by using mechanical friction. It is likely that this mechanical friction causes some problems in real-life systems, such as abrasion of the attaching device and friction-induced vibrations due to its slip. Moreover, in a real system, it might be hard to make the local vibration of the secondary spring disappear within a short period of time before the next attachment. In other words, the mechanical variable-stiffness actuator makes it difficult to minimize an idle duration time Δt_m, so the performance of the mechanical actuator is limited. Therefore, the first objective of this paper is to propose a method of realizing this MED actuator by using a piezoelectric transducer and electric devices. This proposed actuator has electrical energy-dissipation mechanism that imitates the mechanical one. Since, in general, electricity can change its state much faster than mechanical motion, it is possible that the idle duration will be reduced and accordingly the performance of the variable-stiffness actuator will be enhanced.

Recently, some studies on closed-loop vibration controls by using electric devices based on an energy-recycling approach have been reported (Richard *et al.* 2000, Corr and Clark 2002, Onoda *et al*. 2003). The energy-recycling system called SSDI, LR-switching. RL-shunt, and so forth, depending on switching strategy. This approach has been used in many applications (Ji *et al.* 2009a, Ji *et al*. 2009b). A latest overview of this field (i.e., switching control approach using piezoelectric materials for vibration suppression) was presented (Qiu *et al*. 2009). These papers addressed the superiority of the energy-recycling approach to the energy-dissipative approach. Therefore, as the second object of this paper, an electrically-induced variable-stiffness actuator based on the energy-recycling approach is discussed and compared with the energy-dissipation actuator from the viewpoint of open-loop vibration control.

This paper presents in-depth discussion and insight on electrically-induced variable-stiffness actuators by analyzing their performances in open-loop vibration control. The investigations make a comprehensive evaluation of open-loop actuation methods, and pave the way for their practical applications in actual structures.

4. Variable-stiffness actuator using electric devices

4.1 Mathematical model of piezoelectric transducer

Fig. 3 shows a commercially available piezoelectric transducer (ASB171C801NP0, NEC/TOKIN Co.) having a length of 0.22 m, and a mass of 93 g. As the Fig. shows, it consists of a piezoceramic stack, an armoring metal on the outside, and attached fittings. The armoring metal covers the piezoceramic stack to exert pre-compressed force on it, and to protect it from surrounding atmosphere, such as humidity. The piezoelectric stack is a pile of with thin piezoelectric layers. We focus on the longitudinal behavior of the piezoelectric transducer. The relation between applied tensile force f_p, elongation u_p, piezoelectric voltage V_p and stored electric charge Q_p can be written as

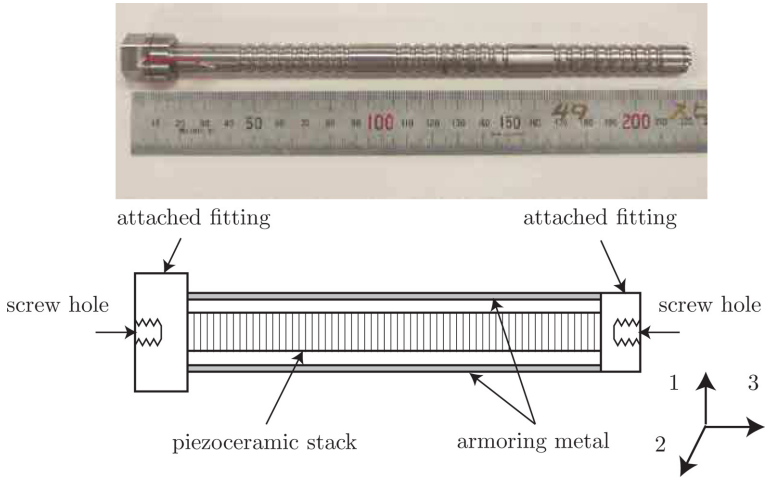

Fig. 3 An example of piezoelectric transducer (above) and mechanical structure (below)

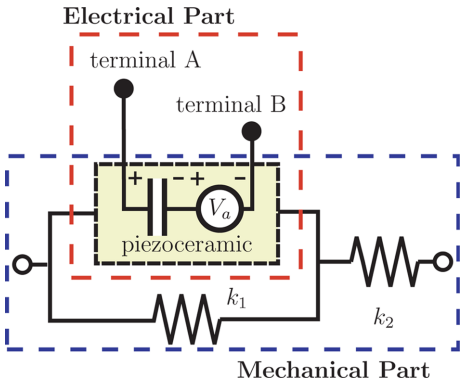

Fig. 4 Mechanical and electrical parts of mathematical model of piezoelectric transducer

$$f_p = k_p u_p - b_p Q_p, \quad V_p = -b_p u_p + \frac{Q_p}{C_p^s} \tag{5}$$

where k_p is the constant-charge stiffness, b_p is the piezoelectric coupling coefficient, and C_p^S is the constant-elongation capacitance of the piezoelectric transducer (Jaffe *et al.* 1991). In Fig. 4, the piezoelectric transducer has two electric terminals A and B, and the voltage difference between A and B is V_p. In Eq. (5), the electrical part of the piezoelectric transducer is modeled with a capacitor and $V_a(=-b_p u_p)$ due to the piezoelectric effect. In this study, we assume the linearity of the piezoelectric transducer to clarify its behavior of our actuation systems. So, we adopt the linear Eq. (5) that is used commonly.

In order to prevent terminology confusion, some words in this paper are defined. The electric device in Fig. 3 is called the piezoelectric transducer, instead of the piezoelectric actuator. As will be seen, combined systems composed of piezoelectric transducers and electric circuits are called the actuation system or the electrical actuator. Therefore, upcoming two actuation systems (EED actuator and EER actuator) do not indicate sole piezoelectric transducers, but combined actuation systems that are made up of piezoelectric transducers and electric circuits.

4.2 Electrical energy-dissipation (EED) actuator

This paper proposes a method of realizing the MED actuator by using a piezoelectric transducer. For the convenience of later discussion, a two-mass system model shown in Fig. 5 is used. The piezoelectric transducer is connected to the base and the base mass m_2. Parts other than the transducer and the base mass will be explained later. From Eq. (5), the mathematical model of the transducer can be written as

$$f_{act} = k_p y_2 - b_p Q_p, \quad V_p = -b_p y_2 + \frac{Q_p}{C_p^S} \tag{6}$$

The proposed electrical energy-dissipation (EED) actuator consists of a piezoelectric transducer and an electric circuit I shown in Fig. 6. By controlling the switch, the electrical status of the piezoelectric transducer is changed. In consequence, a variable-stiffness mechanism is achieved by the change of the electrical status in the electric actuator. For the system with the circuit I, it is clear

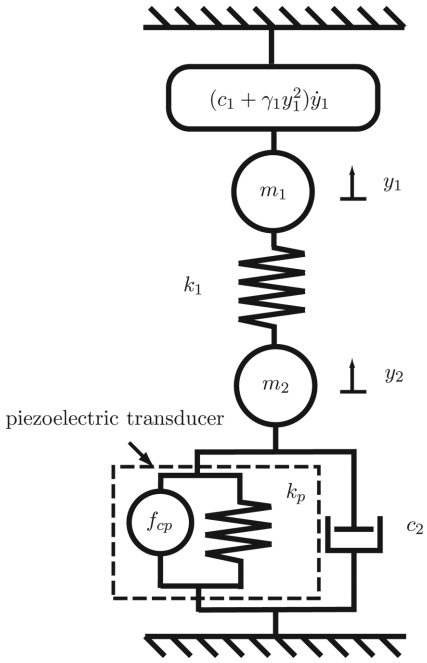

Fig. 5 A two-mass system with piezoelectric transducer subject to self-excitation $(c_1+\gamma_1 y_1^2)\dot{y}_1$. $f_{cp}(=-b_pQ_p)$ represents force generator due to converse piezoelectric effect

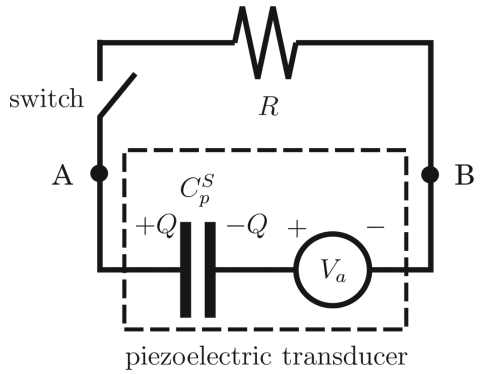

Fig. 6 Electric circuit I for electrical energy-dissipation (EED) actuator

that

(a) when the switch is closed $$R\dot{Q}_p = -V_p \tag{7}$$

(b) when the switch is open $$\dot{Q}_p = 0 \tag{8}$$

By using Eqs. (6) and (7) can be rewritten as

(a) when the switch is closed $$R\dot{Q}_p + \frac{Q_p}{C_p^S} = b_p y_2 \tag{9}$$

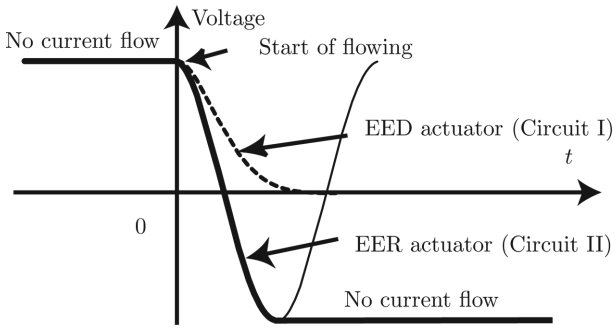

Fig. 7 Transition of piezoelectric voltage after current starts flowing, for EED and EER actuators

By using Fig. 7, the transition of piezoelectric voltage after the switch is closed is explained. It is assumed that electricity changes its state much more rapidly than a structure. In the following discussion, displacement y_2 is assumed to hold a value of y_0 during the quite short period in which electricity changes. The switch is open until $t = 0$. Thus, electric current does not flow before $t = 0$, and starts flowing at $t = 0$. After the switch is closed at $t = 0$, the subsequent transition of Q_p is derived from Eq. (9) as

$$Q_p(t) = b_p C_p^S y_0 + (Q_0 - b_p C_p^S y_0) E^{-\frac{t}{RC_p^S}} \tag{10}$$

where Q_0 is the electric charge at $t = 0$. Since Q_p approaches $b_p C_p^S y_0$ exponentially, V_p approaches 0 exponentially as Eq. (6) indicates. When this short transition of approaching of voltage is neglected, it is valid that V_p=0 after the current finishes flowing. In this case, by eliminating Q_p between Eq. (6) and by substituting $V_p = 0$ into them

$$f_{act} = (k_p - b_p^2 C_p^S) y_0 \tag{11}$$

is obtained. After the current finishes flowing, Q_p keeps a value of $b_p C_p^S y_0$ until the current flows again. Accordingly, the actuator's force is written as

(a) when the switch is closed $$f_{act} = (k_p - b_p^2 C_p^S) y_2 \tag{12}$$

(b) when the switch is open $$f_{act} = k_p y_2 - b_p^2 C_p^S y_0 \tag{13}$$

where y_0 is displacement of the base mass when the current finishes flowing. Comparing Eqs. (12) and (13) with Eqs. (1) and (2), the EED actuator has the same mechanism as the MED actuator in terms of the actuator's force. It is obvious that $k_p = k_a$ and $b_p^2 C_p^S = \varepsilon k_a$. The detachment state of the secondary spring is equivalent to the closed state of the electric switch, and the attachment state is comparable to the open state. This identity of formulations clearly indicates that this electrical energy-dissipation (EED) actuator can be substituted for the mechanical energy-dissipation (MED) actuator.

Since preceding studies dealing with the variable-stiffness piezoelectric actuator have neglected electrical dynamics based on the Kirchhoff equation, the equilibrium point's shift expressed as $-b_p^2 C_p^S$ in Eq. (13) has been ignored. Thus, these studies focused only on the variation of the stiffness value between k_p and $k_p - b_p^2 C_p^S$ in Eqs. (12) and (13). However, in contrast to the conventional analysis,

when electrical dynamics are fully considered together with mechanical dynamics, it proves that the electric charge moves from one side of a capacitor to the other through the electric circuit after the circuit switch is closed. This moving electric charge results in a shift of mechanical equilibrium point. This is the crucial mechanism of the variable-stiffness actuators composed of the piezoelectric transducer and the switchable circuit, which has been neglected.

An open-loop vibration control for the system with the EED actuator is constructed by applying the control notion that leads to the control logic given by Eqs. (3) and (4) for the system with the MED actuator. The control logic for the system with the EED actuator can be written as

the switch is closed	during Δt_{EED} just after $t = 2n\pi / \omega$	(14)
the switch is open	otherwise	(15)

From a practical standpoint, $\Delta t_{EED} \approx 5RC_p^S$ is long enough to ensure the decay of the electrical system expressed by Eq. (10).

While the circuit switch is open, no electric current flows in the circuit. During the period, the mechanical energy of the vibrating structure is converted into electrical energy through the piezoelectric actuator and is stored in the capacitor of the piezoelectric actuator. Every time the switch is closed, the voltage exponentially approaches zero according to Eq. (10), so the electrical energy is dissipated. The piezoelectric voltage resets to be zero when the switch is closed, the absolute value cannot grow. These mechanisms constantly dissipate the converted electrical energy, and consequently decrease the vibration energy. Since the circuit switch is controlled, there is no chance of external energy entering the system. Therefore, this method eliminates the danger of instability, because the total energy of the system decreases monotonically. This is the mechanism of vibration control of EED actuator system.

4.3 Electrical energy-recycling (EER) actuator

As mentioned previously, some studies on closed-loop vibration controls by using electric devices based on an energy-recycling approach have been reported (Richard *et al*. 2000, Corr and Clark 2002, Onoda *et al.* 2003). An electrically-induced variable-stiffness actuator based on the energy recycling approach is also discussed. Hereafter, this actuator is referred to as an electrical energy-recycling (EER) actuator. The combination of a piezoelectric transducer and a circuit II shown in Fig. 8 is used for this actuator. It is clear that

(a) when the switch is closed	$L\ddot{Q}_p + R\dot{Q}_p = -V_p$	(16)
(b) when the switch is open	$\dot{Q}_p = 0$	(17)

By using Eqs. (6) and (16) is given by

(a) when the switch is closed	$L\ddot{Q}_p + R\dot{Q}_p + \dfrac{Q_p}{C_p^S} = b_p y_2$	(18)

Eq. (18) can be rewritten as

$$\ddot{Q}_p + 2\zeta_c \omega_c \dot{Q}_p + \omega_c^2 Q_p = \frac{b_p}{L} y_2,\ \omega_c \equiv \sqrt{\frac{1}{LC_p^S}},\ \zeta_c \equiv \frac{R}{2L\omega_c} \tag{19}$$

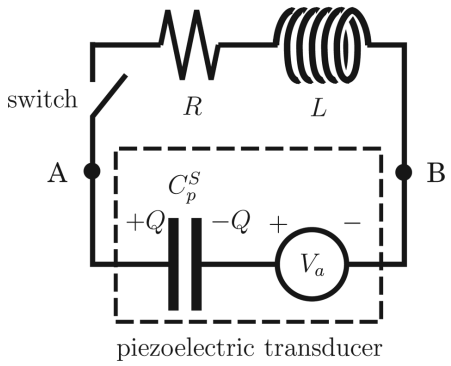

Fig. 8 Electric circuit II for electrical energy-recycling (EER) actuator

The switch of the circuit II is closed at $t = 0$. At this time V_p is V_0, y_2 is y_0, and Q_p is Q_0. By using Eq. (6)

$$V_0 = -b_p y_0 + \frac{Q_0}{C_p^S} \tag{20}$$

is obtained. By solving Eq. (19) for Q_p, an oscillatory solution is obtained $t = 0$

$$Q_p(t) = (Q_0 - b_p C_p^S y_0)\left\{\cos(\omega_c\sqrt{1-\zeta_c^2}t) + \frac{\zeta_c}{\sqrt{1-\zeta_c^2}}\sin(\omega_c\sqrt{1-\zeta_c^2}t)\right\}e^{-\zeta_c\omega_c t} + b_p C_p^S y_0 \tag{21}$$

By assuming that $\zeta_c << 1$, Eq. (21) is simplified into

$$Q_p(t) = (Q_0 - b_p C_p^S y_0)\cos(\omega_c t)e^{-\zeta_c\omega_c t} + b_p C_p^S y_0 \tag{22}$$

From Eqs. (6), (20) and (22)

$$V_p(t) = V_0\cos(\omega_c t)e^{-\zeta_c\omega_c t} \tag{23}$$

is obtained. The transition of voltage after the switch is closed, is illustrated in Fig. 7. After $t = 0$ voltage starts to oscillate, following Eq. (23). Approximately after half a period of electrical vibration, voltage reaches a peak of vibration and its polarity is reversed. If the switch is again opened at this peak, the reverse value of voltage is kept. From Eq. (23), voltage at $t = \pi/\omega_c$ is

$$V_p(\pi/\omega_c) = -V_0 e^{-\zeta_c\pi} \tag{24}$$

In the special case that $\zeta_c = 0$, the absolute value of voltage at $t = \pi/\omega_c$ is exactly the same as that at $t = 0$. This means that the electrical energy stored in the piezoelectric transducer is recycled, rather than immediately dissipated.

An open-loop vibration control for the system with the EER actuator is constructed by applying the same control notion as the EED actuator. The control logic for the system with the EER actuator can be written as

the switch is closed during Δt_{EER} just after $t = 2n\pi/\omega$ (25)
the switch is open otherwise (26)

where

$$\Delta t_{EER} \equiv \frac{\pi}{\omega_c \sqrt{1-\zeta_c^2}} \tag{27}$$

It should be noted that the EER actuator also has a shift of mechanical equilibrium point due to the moving electric charge after the circuit switch is closed.

In EER system, every time the circuit switch is closed, the polarity of piezoelectric charge and voltage reverse because electrical oscillation according to Eq. (21). Consequently the electrical energy is preserved to be used later on, rather than being dissipated immediately. While the switch is open, the mechanical energy is converted to electrical energy and stored in the piezoelectric actuator. These mechanisms increase the electrical energy cumulatively and enable the system to recycle the energy, which is different from the mechanisms in EED actuator system. The piezoelectric voltage and charge reverse in polarity when the switch is closed, the absolute value of piezoelectric voltage can be larger than EED system. The absolute value of piezoelectric voltage in EER system can be higher than that in EED system. We keep in mind that the voltage is regarded as control value in Eq. (31). Because EER system has larger control value than EED system, it can be expected to have better performance.

5. Two-mass model with variable-stiffness actuator

5.1 Mechanical model of two-mass system

A two-mass system with self-excitation as shown in Fig. 5 is considered. The system has a piezoelectric transducer that generates forces expressed by Eq. (6). The top mass m_1 has self-excitation that is modeled as the Van der Pol-type self-exciting force, and is given by

$$f_{se} \equiv (c_1 + \gamma_1 y_1^2)\dot{y}_1 \tag{28}$$

where c_1 is negative and γ_1 is positive. The non-linear equations of motion for the system are

$$m_1\ddot{y}_1 + (c_1 + \gamma_1 y_1^2)\dot{y}_1 + k_1(y_1 - y_2) = 0 \tag{29}$$

$$m_2\ddot{y}_2 + c_2\dot{y}_2 - k_1(y_1 - y_2) + k_p y_2 = b_p Q_p \tag{30}$$

When $y_1 > \sqrt{-c_1/\gamma_1}$, f_{se} acts as a negative damping and can make the system unstable, and when $y_1 > \sqrt{-c_1/\gamma_1}$, f_{se} acts as a positive damping. Therefore, displacements y_1 and y_2 are enclosed by the limit-cycle boundary. The steady-state amplitudes depend on the degree of the instability of the system. By using Eqs. (6) and (30) can be expressed as

$$m_2\ddot{y}_2 + c_2\dot{y}_2 - k_1(y_1 - y_2) + (k_p - b_p^2 C_p^S)y_2 = b_p C_p^S V_p \tag{31}$$

5.2 Discussion of electric variable-stiffness actuators

The state of the EED and EER actuators is changed by opening and closing the switch, so no additional energy is provided to the system. The vibration energy of the system does not increase with the action of the switch. This leads to the significant robustness, which is a great merit of these electric actuation methods.

The crucial difference between the EED and EER actuators can be explained by the transition of piezoelectric voltage after the switch is closed. As can be seen in Fig. 7, voltage of the EED actuator approaches 0 exponentially. In contrast, voltage of the EER actuator keeps a larger absolute value when it stops at an electrical oscillation peak. The voltage value after the electric current finishes flowing is essentially di.erent between these actuators. In the equation of motion expressed by Eq. (31), the voltage value can be regarded as the control input of the system. In general, the control performance is supposed to improve with the increase in the voltage value, as long as the polarity of voltage is suitable for vibration control. In this sense, the EER system should perform better than the EED system.

The difference between the EED and EER actuators can also be interpreted from the perspective of energy. Electrical energy stored in the piezoelectric transducer can be measured with the squared value of piezoelectric voltage (Makihara *et al.* 2007). While the switch is open, mechanical energy is converted to electrical energy because of the piezoelectric effect, and is stored in the piezoelectric transducer. For the EED system, every time the switch is closed, this stored energy is released and dissipated by the resistor in the circuit I. This energy-dissipation mechanism is easily understood with the motion of the secondary spring of the MED actuator. On the other hand, for the EER system, every time the switch is closed and opened after Δt_{EER}, the stored electrical energy is kept rather than being dissipated immediately. Therefore, the converted electrical energy increases cumulatively and enables the EER system to continue to exert high value of force.

In closed-loop vibration controls for a plate (Richard *et al*. 2000), a beam (Corr and Clark 2002) and a truss (Onoda *et al*. 2003), the EER actuation has shown better performance than the EED actuation. However, the superiority of these actuations' merits in terms of the open-loop vibration control cannot be concluded. The performance comparison will be discussed in the section of numerical simulations.

5.3 Transformation of system equation

For a further analysis, it is convenient to introduce dimensionless coordinates and characteristic parameters. Non-dimensional displacements $x_j = y_j/y_{ref}\,(j = 1,2)$ can be de.ned with respect to a reference value y_{ref}.

$$\omega_1 \equiv \sqrt{\frac{k_1}{m_1}}, \quad \tau \equiv \omega_1 t, \quad x_j \equiv \frac{y_j}{y_{ref}}, \quad \eta \equiv \frac{\omega}{\omega_1}, \quad M \equiv \frac{m_1}{m_2} \tag{32}$$

$$d_1 \equiv \frac{c_1}{m_1 \omega_1}, \quad d_2 \equiv \frac{c_2}{m_2 \omega_1}, \quad \gamma \equiv \frac{\gamma_1 y_{ref}^2}{m_1 \omega_1} \tag{33}$$

$$k_p \equiv \frac{M k_p}{k_1}, \quad \beta_p \equiv \frac{M b_p}{k_1}, \quad \phi_p \equiv \frac{V_p}{y_{ref}}, \quad \psi_p \equiv \frac{Q_p}{y_{ref}} \tag{34}$$

Here, ω_1, τ, x_j, η, M are natural frequency of the subsystem, non-dimensional time, non-dimensional displacement of the subsystem j, non-dimensional natural frequency of the subsystem, and mass ratio of two masses, respectively. d_1 and d_2 are non-dimensional damping coefficients, and γ is non-dimensional non-linear damping coefficient. k_p, β_p, ϕ_p, ψ_p are non-dimensional stiffness of the piezoelectric actuator, non-dimensional piezoelectric coefficient, non-dimensional voltage, non-dimensional electric charge, respectively. d_1 and d_2 are related to the linear dashpot elements, while γ is related to the non-linear damping that comes from the self-exciting force in Eq. (28). All parameters with subscript p are non-dimensional values of the piezoelectric actuator in our considered system.

The non-dimensional equations of motion of the two-mass system are given by

$$x_1'' + (d_1 + \gamma x_1^2)x_1' + (x_1 - x_2) = 0 \tag{35}$$

$$x_2'' + d_2 x_2' - M(x_1 - x_2) + k_p x_2 = \beta_p \psi_p \tag{36}$$

The two-mass system has two natural undamped frequencies

$$\Omega_1 \equiv \sqrt{\frac{1}{2}(1 + M + k_p) - \frac{1}{2}\sqrt{(1 + M + k_p)^2 - 4k_p}} \tag{37}$$

$$\Omega_2 \equiv \sqrt{\frac{1}{2}(1 + M + k_p) - \frac{1}{2}\sqrt{(1 + M + k_p)^2 - 4k_p}} \tag{38}$$

5.3.1 Electrical energy-dissipation (EED) actuator

From Eqs. (8), (9), (14) and (15), the open-loop control logic for the EED actuator is

$$\psi_p' + e_1 \psi_p = e_2 x_2 \quad \text{during } \Delta\tau_{EED} \text{ just after } \tau = 2n\pi/\eta \tag{39}$$

$$\psi_p' = 0 \quad \text{otherwise} \tag{40}$$

where

$$e_1 \equiv \frac{1}{RC_p^S \omega_1}, \quad e_2 \equiv \frac{b_p}{R\omega_1} \tag{41}$$

5.3.2 Electrical energy-recycling (EER) actuator

From Eqs. (17), (18), (26) and (27), the open-loop control logic for the EER actuator is

$$\psi_p'' + e_3 \psi_p' + e_4 \psi_p = e_5 x_2 \quad \text{during } \Delta\tau_{EER} \text{ just after } \tau = 2n\pi/\eta \tag{42}$$

$$\psi_p' = 0 \quad \text{otherwise} \tag{43}$$

where

$$e_3 \equiv \frac{R}{L\omega_1}, e_4 \equiv \frac{1}{LC_p^S \omega_1^2}, e_5 \equiv \frac{b_p}{L\omega_1^2} \tag{44}$$

6. Numerical simulation

To investigate the open-loop vibration control performance of the EED and EER systems, numerical

Table 1 Parameter values for simulations

M	variable	d_1	-3.0×10^{-2}	d_2	5.0×10^{-1}
γ	3.0×10^{-4}	k_p	6.0	β_p	3.6×10^{-1}
e_1	5.0×10^{4}	e_2	1.5×10^{4}	e_3	2.2×10^{2}
e_4	1.0×10^{6}	e_5	1.5×10^{6}	-	-

simulations were performed using the two-mass model (see, Fig. 5). The parameter values listed in Table 1 were used in the simulations. The initial condition of vibration was $x_1 = x_2 = x_1' = x_2' = 1.0 \times 10^{-2}$ and $\phi_p = \psi_p = 0.0$. These parameter values were based on our previous paper (Makihara *et al.* 2005). The values for the piezoelectric transducer were determined by referring to a commercially available one (NEC/TOKIN ASB171C801NP0) in Fig. 1. Electric values were based on real devices. Thus, all parameter values were realistic.

6.1 Stability analysis

Fig. 9 shows maximum amplitudes of x_1 after reaching steady conditions, as a function of control frequency η for a mass ratio of $M = 5.0$. The amplitude level of $x_1 \approx 10$ is provided by the system with no control. The EED system fully suppresses the vibration in the interval of η from 0.5 to 4.8, while the EER system fully suppresses the vibration in the interval of η from 0.5 to 1.5, except for a sharp spike. This wide range of fully suppressed frequency η shows that the proposed system is quite robust against the variation of frequency. In reality, due to temperature and aging, the frequency can slightly vary little by little. Considering these realistic condition, this robustness of our systems is quite significant. The EED system has a wider range of stable region than the EER system has. This superiority is in conflict with the conclusion of closed-loop vibration controls (Richard *et al.* 2000, Corr and Clark 2002, Onoda *et al.* 2003). This contradicted conclusion suggests that this open-loop vibration control is essentially different from those closed-loop vibration controls. The simplistic way of reasoning from conclusions of closed-loop methods can lead to critical mistakes in

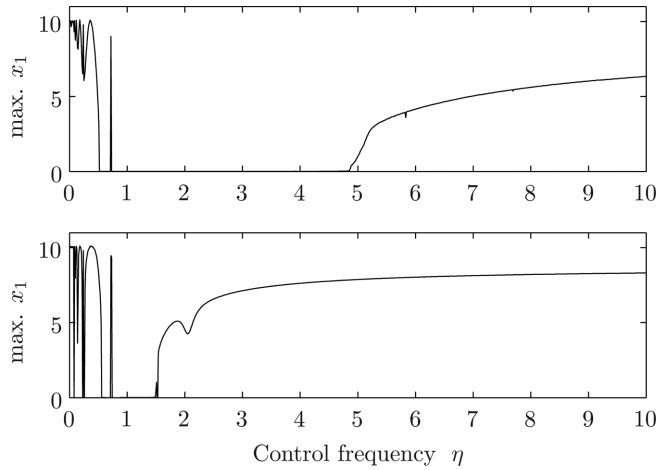

Fig. 9 Range for maximum amplitudes x_{1_max} as a function of control frequency η with M=5.0. Above: EED actuator, below: EER actuator

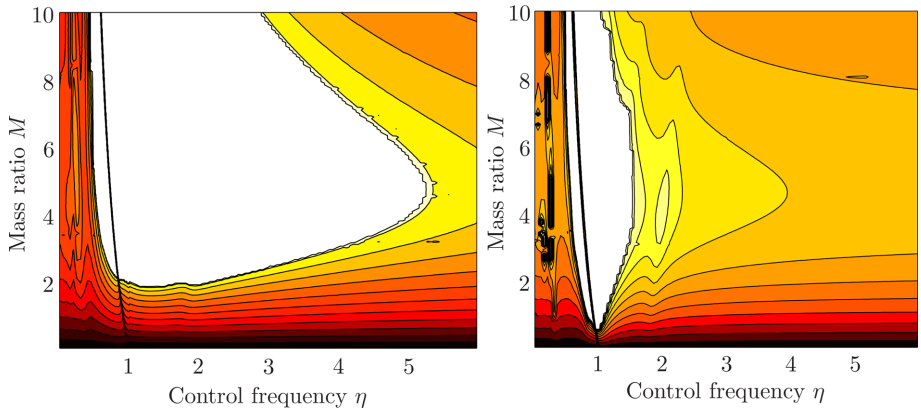

Fig. 10 Maximum amplitudes x_{1_max} as a function of control frequency η and mass ratio M. Left: EED actuator, right: EER actuator

estimating the open-loop control performance.

Fig. 10 shows contour-plots of maximum amplitudes x_1 as a function of η and M. The white region represents the stable area where x_1 is 0 at steady conditions. The darker region indicates a larger amplitude of x_1, meaning less stability of the system. A steep mountain range is visible in the region of $\eta = 0.5$ to 1.0 in the stable region. This range represents the parametric resonance caused by the excitation with frequency $\eta = \Omega_1 = 0.72$. The peak has curved shapes because Ω_1 is a nonlinear function of M. This parametric resonance is discussed profoundly in previous studies (Tondl 1998, Ecker and Pumhossel 2009). It should be noted that, in contrast to the open-loop vibration control using parametric excitations, the vibration amplitude of these EED and EER actuators cannot be worse than that with no control (i.e., $x_1 \approx 10$) even if systems come to the worst. This robustness and reliability of the EED and EER actuators is worth emphasizing for open-loop vibration control.

Fig. 11 shows contour-plots of maximum amplitudes x_1 as a function of η and damping coefficient d_2 with $M = 5.0$. The sharp resonance region where the system is unstable at the frequency $\eta = \Omega_1 = 0.72$ can be seen. When the value of the damping coe.cient d_2 decreases, the system generally becomes unstable. The critical damping coe.cient can be determined by the

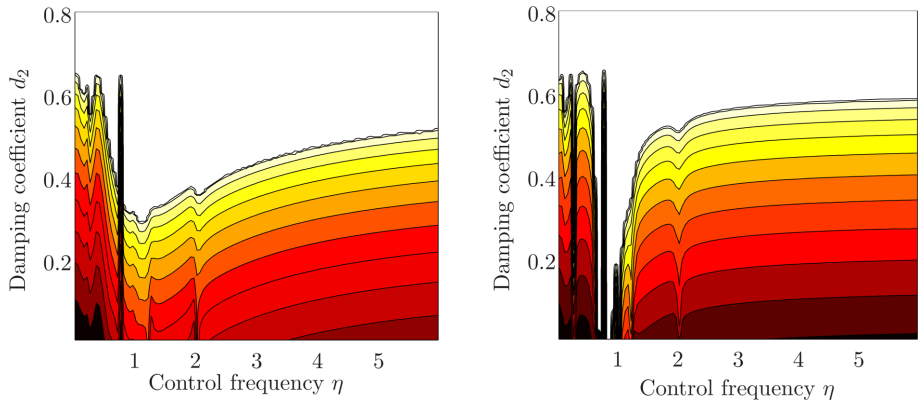

Fig. 11 Maximum amplitudes x_{1_max} as a function of control frequency η and damping coefficient d_2. Left: EED actuator, right: EER actuator

boundary where the system changes its stability. The EED system gives wider combination of η and d_2 for the system's stability, which is consistent with the conclusion obtained from Figs. 9 and 10. Figure 11 indicates that $\eta = 1.12$ is best for the EED system, and $\eta = 0.80$ is best for the EED system, in order to obtain each smallest value of the critical damping coe.cient. However, in the interval of η between 0.8 and 1.3, the EER system provides a small value of the critical damping coefficient. In this interval of η, the control performance of the EER system is much better than that of the EED system. The significantly small value of the damping coefficient is highly remarkable. This can be a great advantage in an actual design where su.cient damping is hard to achieve. From this perspective, the EER actuator promises to be a powerful actuation mechanism, and it is helpful for open-loop vibration control. In summary, the EER and EED systems have both advantage and disadvantage, thus they should be chosen for the purpose of the application of open-loop vibration control.

6.2 Performance analysis of electric actuators

The general control uses both the phase margin and the gain margin for the purpose of measuring the degree of stability. Here, we measure the degree of stability for our actuation system. The direct velocity feed-back control (Balas 1979) indicates that ψ_p should be $-K_f \dot{x}_2$, in order to suppress vibrations of the system expressed by Eqs. (35) and (36). K_f is generally called as the feedback gain and ought to be a positive value. The open-loop vibration control using the EED and EER actuators cannot manipulate the value of ψ_p as desired. However, when ψ_p has the same polarity as $-\dot{x}_2$, it may be possible to speculate that the state of these EED and EER actuators is suitable for the vibration suppression. To investigate the open-loop performance from this viewpoint, a performance index.

$$J \equiv \frac{1}{T_E} \int_0^{T_E} \operatorname{sign}(-\dot{x}_2 \psi_p) dt \tag{45}$$

is calculated where T_E is the termination time when the vibration reached steady state conditions. When J is larger, the control performance is thought to be higher.

Fig. 12 shows the performance index J as a function of η for $M = 5.0$, where the direction of the vertical axis is reversed. Compared with Fig. 9, the similarity of curves' trends can be easily seen. Moreover, Fig. 12 provides additional information of control performance that Fig. 9 has not given. It turns out that Fig. 9 plots a part of the curves which are above the dashed lines in Fig. 12. With Fig. 12, the degree of the stability of the system in the stable interval of η can be discussed and judged. This Fig. suggests that $\eta = 1.12$ is best for the EED system, and $\eta = 0.80$ is best for the EED system. This suggestion on the best value of η completely agrees with the conclusion obtained from Fig. 11. The performance index J is helpful for knowing the degree of stability of the system, which lead to the determination of open-loop frequency η. But J does not take into consideration the amplitude of ψ_p as an actuation performance. As discussed in section 5.2, the control performance is supposed to improve with the increase in ψ_p and ϕ_p. Further discussion taking this viewpoint into consideration is beyond the scope of this paper and is future work.

We finally explain how η is changed in actual systems. η is the non-dimensional natural frequency of the control actuator, which comes from ω. Detailed definition of η and ω is expressed in our previous paper (Makihara *et al*. 2005). η and ω are the variation frequencies of the open-loop control that are expressed in Eqs. (14) and (25). In detail, η or ω is the switching frequency that determines the circuit-closed period of electric circuits for both EED and EER actuators. In actual structural systems with

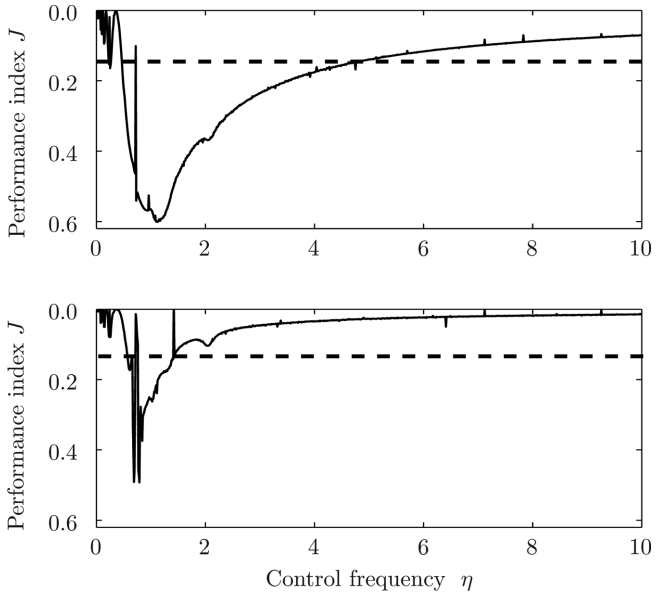

Fig. 12 Performance index J as a function of control frequency η with M=5.0. Above: EED actuator, below: EER actuator

piezoelectric actuators, the value of η or ω is pre-determined in advance of controlling, because our control is based on the open-loop control scheme. These values are input to a frequency oscillator or a function generator of the structures that are subject to self-excitation force. These frequency oscillators and function generators are connected to the circuit switch of EED and EER actuation systems, to control the switch status (i.e., open or close position).

7. Conclusions

In this paper, we proposed an electric variable-stiffness actuator that exploits the electrical mechanism. This proposed actuation system was composed of a piezoelectric transducer and an electric circuit having a switch. It was proven that a variable-stiffness mechanism can be achieved on the electric actuator, only by controlling the switch.

Since, in this paper, electrical dynamics were fully considered together with mechanical dynamics, it proved that the electric charge moves through the circuit, and consequently the mechanical equilibrium point shifts. This paper pointed out the importance of the equilibrium point's shift, while conventional piezoelectric variable-stiffness actuators featured the variation of the stiffness value. Importantly, we focused on the essence of the equilibrium shift, which has been neglected so far.

A two-mass system subject to self-excitation forces was considered to investigate an open-loop vibration control employing this electrical energy-dissipation (EED) actuator. Moreover, an electrical energy-recycling (EER) actuator was also discussed and compared with the EED actuator. Extensive numerical simulations provided comprehensive assessment on both electrically-induced variable-stiffness actuators employed for open-loop vibration control. The EED system provided a wider range of parameter values for the system's stability, which led to robustness and reliability of the system. Meanwhile the EER system provided a more powerful performance with certain combination of

parameter values. These investigations gave insight and fundamental understanding of the open-loop vibration control method using electric devices.

References

Balas, M.J. (1979), "Direct velocity feedback control of large space structures", *J. Guid. Control Dynam*., **2**(3), 252-253.

Clark, W.W. (2000), "Vibration control with state-switched materials", *J. Intel. Mat. Syst. Str*., **11**(4), 263-271.

Corr, L.R. and Clark, W.W. (2002), "Comparison of low-frequency piezoelectric switching shunt techniques for structural damping", *Smart Mater. Struct*., **11**(3), 370-376.

Cunefare, K.A., Rosa, S.D., Sadegh, N. and Larson, G.D. (2000), "State-switched absorber for semi-active structural control", *J. Intel. Mat. Syst. Struct*., **11**(4), 300-310.

Ecker, H. and Pumhossel, T. (2009), "Experimental results on parametric excitation damping of an axially loaded cantilever beam", *Proceedings of the ASME Int. Design Eng. Tech. Conf*.

Jaffe, B., Cook, Jr. W.R. and Jaffe, H. (1971), *Piezoelectric Ceramics*, Academic Press, London.

Ji, H., Qiu, J., Badel, A. and Zhu, K. (2009a), "Semi-active vibration control of a composite beam using an adaptive SSDV approach", *J. Intel. Mat. Syst. Struct*., **20**(4), 401-412.

Ji, H., Qiu, J., Badel, A. Chen, Y. and Zhu, K. (2009b), "Semi-active vibration control of a composite beam by adaptive synchronized switching on voltage sources based on LMS algorithm", *J. Intel. Mat. Syst. Struct*., **20**(8), 939-947.

Kurdila, A.J., Feng, Y. and Lesieutre, G.A. (2000), "Hybrid system stability and capacitive shunting of piezoelectric stiffness", *Proceedings of the ASME Adaptive Struct. Mater. Eng. Systems*, American Soc. Mech. Eng., Fairfield, NJ.

Larson, G.D. and Cunefare, K.A. (2004), "Quarter-cycle switching control for switch shunted dampers", *J. Vib. Acoust*., **126**(2), 278-283.

Makihara, K., Ecker, H. and Dohnal, F. (2005), "Stability analysis of open-loop stiffness control to suppress selfexcited vibrations", *J. Vib. Control.*, **11**, 643-669.

Makihara, K., Onoda, J. and Minesugi, K. (2007), "Comprehensive assessment of semi-active vibration suppression including energy analysis", *J. Vib. Acoust*., **129**(1), 84-93.

Onoda, J., Endo, T., Tamaoki, H. and Watanabe, N. (1991), "Vibration suppression by variable-stiffness members", *AIAA J*., **29**(6), 977-983.

Onoda, J., Makihara, K. and Minesugi, K. (2003), "Energy-recycling semi-active vibration suppression by piezoelectric transducers", *AIAA J*., **41**(4), 711-719.

Qiu, J., Ji, H. and Zhu, K. (2009), "Semi-active vibration control using piezoelectric actuators in smart structures", *Front. Mech. Eng. China*, **4**(3), 242-251.

Ramaratnam, A. and Jalili, N. (2006), "A switched stiffness approach for structural vibration control: theory and real-time implementation", *J. Sound Vib*., **291**(1-2), 258-274.

Richard, C., Guyomar, D., Audigier, D. and Bassaler, H. (2000), "Enhanced semi passive damping using continuous switching of a piezoelectric device on an inductor", *Proceedings of the SPIE Conf. on Damping and Isolation*, Newport Beach.

Tondl, A. (1998), "To the problem of quenching self-excited vibrations", *Acta Technica CSAV*, **43**(1), 109-116.

Tondl, A. and Ecker, H. (2003), "On the problem of self-excited vibration quenching by means of parametric excitation", *Arch. Appl. Mech*., **72**(11-12), 923-932.

CC